JOURNAL OF THERMOPHYSICS AND HEAT TRANSFER
Vol. 10, No. 3, July–September 1996

Thermal Control System for Lunar Base Cooling

K. R. Sridhar* and Matthias Gottmann†
University of Arizona, Tucson, Arizona 85721

The design of a thermal control system (TCS) for cooling a lunar base is considered. Conventional techniques cannot be used for this purpose because of the lack of a readily available heat sink during most of the lunar day. The temperature of the lunar surface near the equator reaches a maximum of about 390 K during the lunar day. The projected range of temperatures for operation of sensors and thermally conditioned habitat spaces is 270–293 K. A heat-pump-augmented TCS can be used to increase the operating temperature of the radiator, thereby enabling heat rejection. The masses of TCSs utilizing Rankine cycle and closed Brayton cycle heat pumps are examined in detail. The TCSs are optimized for minimum total mass. Quantitative comparisons show that the Rankine cycle systems are less massive than the Brayton cycle systems. The optimal total TCS mass for a Rankine cycle heat pump with R11 as the heat pump working fluid and R717 in the rejection loop is 5940 kg at a rejection temperature of 362 K. Sensitivity analyses are performed for radiator-specific mass and power penalties.

Introduction

A DESIGN for a thermal control system (TCS) that is capable of cooling a permanently inhabited lunar base is presented. Moderate-temperature heat (278–293 K) is to be removed from an outpost on the moon designed to house a crew of six humans and operate for over 10 years continuously. Thermal control systems are essential for maintaining temperatures within acceptable levels in the various subsystems of any spacecraft or space-based facility. The complex and miniaturized spacecraft of the future pose difficult thermal design problems and will involve sophisticated active control equipment. The excess heat is rejected from the craft into space by radiative heat transfer. A temperature differential between the radiator and the environment of 40–50 K is a practical minimum for a radiator to be of reasonable size. For most applications, a thermal sink that is significantly cooler than the radiator is readily available in space. The lack of a low-temperature thermal sink makes the lunar base thermal cooling problem technically challenging.

The variation of temperature on the lunar surface in areas near the equator is shown in Fig. 1. Almost all desired locations for the frontier lunar bases are in close proximity to these equatorial regions, where the surface temperature peaks at about 390 K during the lunar day. The direct dissipation of waste heat from the lunar base is not possible given the adverse temperature gradient.

Several techniques for moderate-temperature thermal control on lunar bases have been proposed, such as lunar soil thermal storage, parabolic-shaded radiators, and heat pumps.[2–5] The effect of the lunar environment on the performance of the critical components of all the proposed systems is largely unknown. In the thermal storage concept,[4] the excess heat from the base is pumped down, using a working fluid, to a heat exchanger buried deep under the lunar surface. The cool lunar soil provides the necessary low-temperature sink. The large-scale excavation deep into the surface of the moon and a lack of knowledge about the thermal properties of the lunar soil deep under the surface pose implementation and design problems. The concept of shaded lightweight radiators has been proposed.[6] Shielding the radiator from the hot lunar soil could radically decrease the radiator operating temperature.[6] The shade must be made of specular material and the degradation rate of specular properties with time in the lunar environment is not known. Also, the fine dust kicked up from the surface around the base would have a serious impact on performance. At least for the frontier bases, a prudent approach would be to employ systems that rely on proven terrestrial technology and are least affected by exposure to the lunar environment. The concept of using heat pumps meets these criteria. In this concept, energy is supplied to the heat pump to transport heat from a low-temperature lunar base to a radiator at a much higher temperature. The temperature lift provided by the heat pump is sufficient for a reasonably sized radiator to dissipate the waste heat. The heat pump concept is also somewhat dependent on the degradation rate of the radiator surface properties with time, but much less so than the shaded radiator concept. The heat pump concept will be pursued in this article. A simple schematic of a heat-pump-based TCS is shown in Fig. 2.

Note that, while they are not commonplace, there are many space applications, in addition to a lunar base, where a heat-pump-augmented thermal control system would be beneficial. All situations where a thermal sink with a 40–50 K temperature differential is not readily available would be candidates for the heat-pump-based TCS. Examples include lunar rovers that have long life expectancies and a Mars lander with high heat flux dissipation (the predominantly carbon dioxide atmosphere and the dust loading would make radiation difficult). With the miniaturization of spacecraft subsystems and the push toward smaller spacecraft, the heat pump TCS would allow for compact radiators. The compact radiators would also be attractive for military applications.

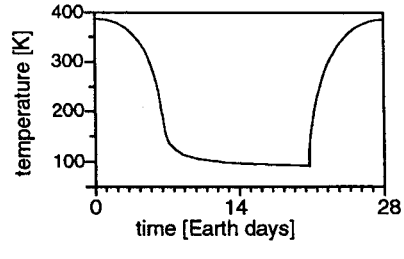

Fig. 1 Temperature variation of the lunar surface at the equator.[1]

Received Feb. 9, 1995; revision received Jan. 23, 1996; accepted for publication Jan. 24, 1996.

*Assistant Professor, Department of Aerospace and Mechanical Engineering. Senior Member AIAA.

†Graduate Research Assistant, Department of Aerospace and Mechanical Engineering.

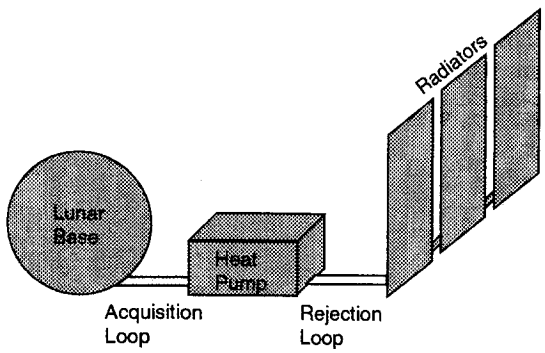

Fig. 2 Schematic of a heat-pump-based TCS.

Heat Pump Considerations

Several different concepts for heat-pump-based TCS for the lunar base can be envisioned. It is possible to have a central thermal bus, with heat pumps located at the radiator, or to have a distributed thermal bus, with heat pumps located at the load sources. A combination of the two concepts is also possible. While both concepts have their inherent advantages and disadvantages, it has been shown that a single centralized thermal bus system is better from a mass standpoint.[4] Hence, the centralized concept will be considered in this article.

Heat pumps have been used for terrestrial applications, such as air conditioning and refrigeration, for a long time. For large thermal loads, heat pumps operating on the Rankine, absorption, or Brayton cycles have been used. The most common cycle for terrestrial applications is the Rankine cycle, also called the vapor compression cycle. Absorption cycles differ from the Rankine cycle by requiring that heat energy, not shaft work, provide the temperature lift for the heat flux. Brayton cycle heat pumps utilize a gas coolant rather than a phase-change material. Stirling cycle heat pumps have been employed for cryogenic temperature ranges and low heat loads. In this article, the Rankine cycle heat pump is analyzed as a baseline system, followed by an analysis of the Brayton cycle.

Both the Rankine and Brayton cycle heat pumps are work-driven heat pumps since they require shaft work to operate. Absorption heat pumps are heat driven and are often used in terrestrial applications when sources of waste heat are readily available, for example, from power or chemical plants. It would appear that the availability of solar heat on the moon would make such units attractive for lunar base cooling. However, plenty of moderate-temperature heat needs to be rejected from such a heat pump and this more than offsets the advantage offered by solar heat. Ammonia–water and water–lithium bromide absorption heat pumps have been evaluated by the authors for their suitability. They found that these heat pumps are not competitive compared with the Rankine and Brayton systems. For this reason, absorption heat pumps will not be discussed in this article; the interested reader can find details in Ref. 7.

To optimize the mass of the heat-pump-based TCS, all promising options have to be evaluated and compared. This comparison requires the careful choice of system operating parameters, working fluids, and component masses. As with all comparative studies, a common yardstick will be the basis on which the different systems will be compared. For space applications, the total mass of a system is a good parameter. The single largest fraction of any space mission is the launch cost from Earth. For this optimization study, total mass of the TCS will be the objective function that will be minimized. For simplification purposes, the following assumptions are made: the systems are modeled for full-load operation, and the implications and power penalties at off-design and part-load conditions are not considered. However, the surface temperature of the lunar regolith varies from 80 to 390 K during the lunar day. This variation in the regolith temperature indicates that the temperature lift and total heat dissipated would vary as a function of the time of day. For this reason, the performance of the heat pump at partial-load conditions is important and will be studied in detail in the future. Note that, for mass optimization and comparison of systems, the peak heat loads and peak power requirements are the relevant metrics. While evaluating system mass, the mass of the control components is not accounted for since the control system masses for the various concepts do not vary significantly and their absolute mass is very small in comparison to the total TCS mass. Redundancy requirements are also not considered here.

Problem Definition

Rankine and Brayton cycle heat pumps are considered for moderate-temperature heat rejection from a lunar base. Analysis is performed to find the optimal system based on a criterion of least total mass. The base, designed for four to eight crew members, is presumed to have an electrical consumption of 100 kW. It is also assumed that this base is located in an equatorial region of the moon. The cooling load and the acquisition temperature are described next.

Several studies have estimated the electrical power input of a lunar base to be about 100 kW.[3,4,8] To protect the crew and equipment from harsh radiation and from micrometeoroid impact, the walls are made of thick, insulating material and the net heat exchange with the outside environment through the walls is negligible. The metabolic heat generated by the crew members (~150 W/crew member) is negligible in comparison with that generated by the electrical input. It is assumed that the net thermal mass within the lunar base does not vary significantly with time and that all of the electrical energy is finally dissipated as heat. Based on these considerations, the total cooling load for the lunar base is fixed at 100 kW.

The acquisition loop collects the excess heat from the base and transports it to the heat pump. For safety reasons, a chilled water loop will be used to acquire and transport the heat to the heat pump within the habitable regions of the base. Nontoxic trace additives may be added to water to depress its freezing point. For this study, it was decided that a single cooling loop operating at 275 K, the lower of the two Space Station cooling loop temperatures, would be used. The variation of the temperature of the coolant in the acquisition loop has to be chosen such that, for a reasonable mass flow rate of coolant, the given cooling load can be handled. With water as the coolant and a 5-K variation in temperature, the mass flow rate of the coolant in the acquisition loop would be 4.8 kg/s.

Rankine Cycle Heat Pump

A study was conducted to optimize a heat pump operating on a Rankine cycle. Two different configurations were considered. In the first, termed case A, the heat pump is directly connected to the rejection loop. In this configuration, the condenser of the heat pump and of the radiator are one and the same, leading to mass savings. In this case, there is only one fluid flowing through the heat pump and radiator. Figure 3 depicts a simple schematic of this configuration. Figure 4 is a schematic for case B, where the condenser of the heat pump exchanges heat with a coolant in a rejection loop connected to the radiator. In addition to adding extra components to the system, this configuration also imposes pressure and temperature-drop penalties on the system. However, this configuration offers very attractive operational advantages. In case B, it is relatively easy to connect several modular heat pumps in parallel without concern about proper flow distribution. The accidental loss of refrigerant on one side of the condenser will not affect the other side, thereby enhancing the survivability of the overall system. In addition, repairability and incorporation of redundancy requirements are much improved. This concept also may be particularly valuable should the radiator

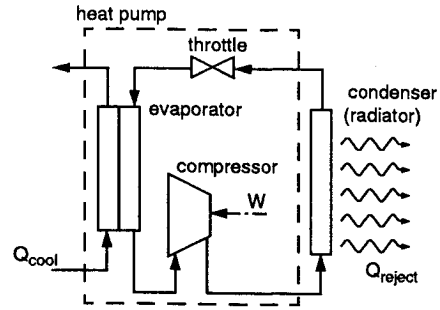

Fig. 3 Rankine cycle heat pump configuration, case A.

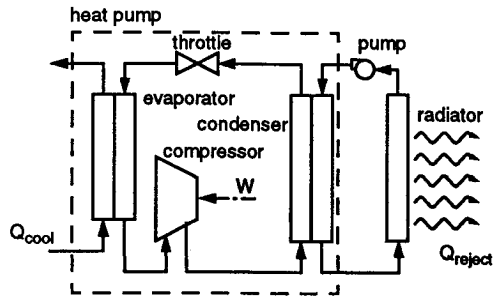

Fig. 4 Rankine cycle heat pump configuration, case B.

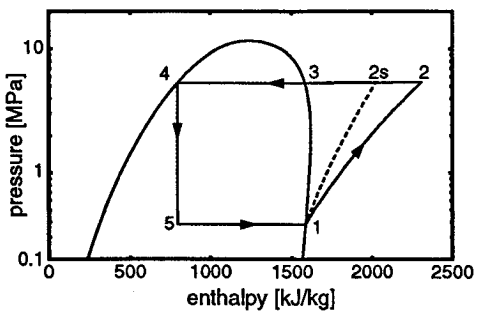

Fig. 5 Pressure-enthalpy diagram for a Rankine cycle heat pump.

and/or transport lines prove susceptible to micrometeoroid damage.

Figure 5 is a pressure-enthalpy diagram for the Rankine cycle. A compressor pressurizes the working fluid from state 1 to state 2. The working fluid is cooled in a condenser from state 2 to state 4, followed by expansion in a throttle valve to state 5. Low-pressure liquid vaporizes in an evaporator and attains state 1.

Compressor

The working fluid in the vapor state is compressed from state 1 to state 2 by the compressor. Ideally, this process would be isentropic (1–2S), but in reality it is nonisentropic (1–2) because of the irreversibilities. The properties of the refrigerants used in the modeling are real properties, which were obtained from an in-house computer database generated using TPSI handbook data.[9] Deviations from the ideal behavior in the compression occur because of mechanical, electrical (motor), and electronic (controller) inefficiencies, and fluid friction. In state-of-the-art aircraft compressors of comparable size, the overall efficiency is $\eta_{total} = 0.61$. Since the compressor would be located outside the thermally conditioned space and the radiation losses from the compressor surfaces are negligible, all of the energy supplied to the compressor goes into compressing and heating the refrigerant. The mass of a state-of-the-art compressor for aircraft applications is 0.45 kg for every kilowatt of cooling load. In our application, the cooling load will remain the same (100 kW) during the mass optimization, but the rejection heat load will vary, depending on the temperature lift. An analysis was performed to obtain a compressor specific mass of 0.202 kg for every kilowatt of rejected heat.[10]

Condenser

Between states 2 and 3, the compressed, superheated vapor cools to saturated vapor, and between 3 and 4 it condenses to saturated liquid. Ideally, this process would be isobaric, but because of pipe friction and configuration changes in the condenser (such as elbows and bends), a small pressure drop will occur. In case A, processes 2 to 3 and 3 to 4 occur in the radiator, since the radiator and condenser are one and the same. The mass of the radiator and the mass of the plumbing from the compressor (heat pump) to the radiator will be discussed later. In case B, the condenser is a heat exchanger separating the heat pump from the rejection loop. A specific mass of 2.72 kg for every kilowatt of heat transferred is assumed for this two-phase heat exchanger.[4] The temperature difference across the two flows in the condenser is set to 5 K, and a pressure drop equivalent to a 1-K temperature drop in each flow loop through the condenser is assumed.

Throttle Valve and Evaporator

Between states 4 and 5, the refrigerant is throttled. The process is assumed to be adiabatic. The mass of a throttle valve is negligible in comparison to the masses of the other components of the heat pump. From state 5 to state 1, the refrigerant absorbs heat from the coolant circulating in the acquisition loop of the lunar base. The absorption of the cooling load takes place in the evaporator. This process deviates from the ideal isobaric process because of a frictional pressure drop in the condenser (assumed to be equivalent to a 1-K temperature drop). The temperature differential between the coolant in the acquisition loop and refrigerant in the evaporator is set at 5 K. The specific mass of the evaporator is taken to be 2.72 kg for every kilowatt of cooling load.[4]

Rejection Loop

In case A, the plumbing from the compressor (heat pump) to the radiator forms the rejection loop, hence, the rejection loop coolant and the heat pump refrigerant are one and the same. Here, the length of the loop is determined by the height of the radiators and the distance from the heat pump to the radiators.[10] The total pressure drop in the rejection loop is taken to be the equivalent of a 1-K temperature drop,[11] since a large pressure drop in the rejection loop would deteriorate the overall performance of the cycle. The diameter of the piping that would permit the specified pressure drop is calculated, and its thickness is set to be the larger of 0.5 mm or the hoop-stress-dictated value with a safety factor of 3. It is assumed that the piping is made of a lightweight, high-strength aluminum alloy with suitable coatings.

In case B, the rejection loop couples the condenser of the heat pump to the radiator and has a mechanical pump to circulate the coolant in the rejection loop. The mass of the pump and its power penalty would have to be taken into account in the mass estimation. The mass and power requirements are computed using the following expressions given by Dexter and Haskin[12]:

$$W_{pump} = \frac{\dot{m}H}{3600 \cdot 550 \cdot \eta} \quad \text{and} \quad M_{pump} = 5.61 \cdot \left(\frac{\dot{m}}{60 \cdot \rho}\right)^{0.75}$$

where W_{pump} is the pump power in horsepower, M_{pump} is the mass of the pump in pounds, $\dot{m}$ is the mass flow rate in pounds per hour, H is the pump head in feet, ρ is the fluid density in pounds per cubic foot, and η is the pump efficiency, which is assumed to be 0.25. The criteria used for pipe thickness, total pressure drop, and pipe mass calculations were the same as in

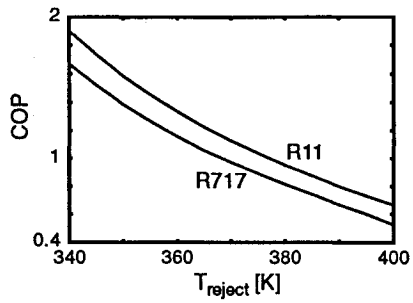

Fig. 6 COP as a function of rejection temperature for R11 and R717.

case A. The coolant used in the rejection loop was R717 because of its superior heat transport characteristics.[10]

Radiator

The function of the radiator is to reject the waste heat from the base. The heat rejected by the radiator is given by

$$Q = A\varepsilon\eta\sigma(T_{\text{reject}}^4 - T_{\text{sink}}^4)$$

where A is the radiator area, ε is the emissivity, η is the fin efficiency, σ is the Stefan–Boltzmann constant, and T_{reject} and T_{sink} are the radiator and sink temperatures, respectively. The estimated peak sink temperature for a vertically mounted radiator at the lunar base is 321 K (Ref. 3). Most sources point to an ε of 0.8 and an η of 0.7 for such radiators. Several widely differing values are reported in the literature for specific masses for radiators.[3,4,13,14] A specific mass of 2.5 kg/m^2 is assumed in the present analysis for vertical two-sided radiators. Recently, radiators with a mass as low as 1.5 kg/m^2 have been demonstrated for lunar base power system applications.[15]

Power Supply

The Rankine cycle requires electric power to provide the shaft work required by the compressor. The capacity of the power station on the lunar base would have to be increased to provide the necessary power. A review of the literature shows that there is no consensus on the mass penalty associated with the power supplies.[3,4,16,17] The values quoted for the SP 100 class nuclear power sources are about 30 kg/kW of electric power. Although the SP 100 program is no longer active, power sources with penalties on the order of 30 kg/kW of electric power would have to be developed to make missions such as lunar habitats feasible. For this reason, a 30 kg/kW power penalty is chosen in this study.

Refrigerants

One of the important issues is the choice of refrigerant for the heat pump. The commonly used vapor compression cycle refrigerants for terrestrial applications are R11, R12, R113, R114, and R717. R113 and R114 were eliminated because of a potential for condensation of the vapor in the compressor. Because of its low critical temperature (385 K) and low coefficient of performance (COP), R12 was not selected. R11 and R717 remained as potential candidates. Using real properties for the refrigerants, the COP of the cycle is computed for a range of rejection temperatures for these two refrigerants and is plotted in Fig. 6.

Closed Brayton Cycle Heat Pump

This section describes the analysis of a TCS concept based on the closed Brayton cycle heat pump. The ideal Brayton cycle consists of two isobaric and two isentropic processes. It uses a compressor, a turbine, and two heat exchangers, and is similar to the Rankine cycle, except that throttling is replaced by an isentropic expansion in the turbine and the working fluid always remains gaseous. These differences point to the inherent advantages and disadvantages of the Brayton cycle. The energy of expansion is not wasted as in a throttling device. Instead, it is recovered in the turbine, thereby reducing the amount of shaft work required. Also, there exists the possibility of using a combined refrigeration and power cycle, which would simultaneously utilize two turbines and one compressor and effectively make use of waste heat that may be available from the power supply subsystem. Since the working fluid remains gaseous throughout the cycle, the mass and volume flow rates are large. The reason is that, on a unit mass basis, the sensible heats are small compared to the latent heats associated with a liquid–vapor phase change. The isobaric heat exchange is not isothermal, and this may cause excessively high compressor and low turbine outlet temperatures, in addition to decreasing cycle performance. Under most conditions, it is advantageous to modify the Brayton cycle using internal heat transfer for heat recuperation. Figures 7 and 8 depict a schematic and temperature–entropy diagram, respectively, of a Brayton cycle heat pump with recuperation. An ideal recuperator, $T_4 = T_6$, is assumed.

The thermodynamic model takes into account the inefficiencies of the components. In real equipment, the compression and expansion cannot be isentropic and heat transfer will not be isobaric. The efficiencies of the compressor and turbine, respectively, are defined by

$$\eta_c = \frac{w_{\text{isentropic}}}{w_{\text{real}}} \quad \text{and} \quad \eta_t = \frac{w_{\text{real}}}{w_{\text{isentropic}}}$$

where $w_{\text{isentropic}}$ is the isentropic work supplied or generated, and w_{real} is the actual work supplied or generated.

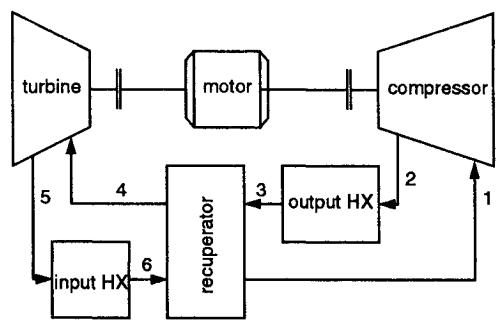

Fig. 7 Schematic of a Brayton cycle with recuperation.

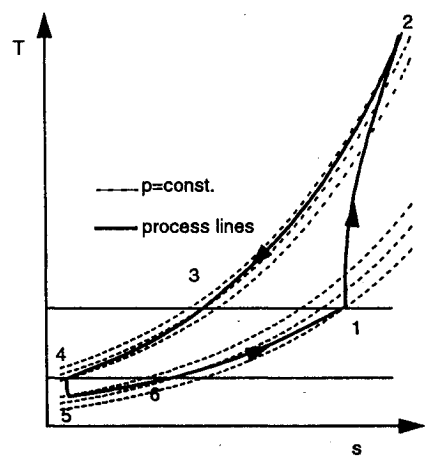

Fig. 8 Temperature–entropy diagram for a Brayton cycle with recuperation.

The heat exchangers and recuperator will be modeled with a relative pressure drop, and the efficiency is defined as

$$\eta_{HX} = (p_{out} - p_{in})/p_{in}$$

where p_{in} is the inlet pressure and p_{out} is the outlet pressure.

The inefficiencies represent a tradeoff between size and mass on the one hand and performance on the other. For this study, values of $\eta_c = 0.8$ and $\eta_t = 0.87$ are assumed. These are the best achievable state-of-the-art efficiencies for the equipment sizes under consideration.

It can be shown that the overall COP is

$$\mathrm{COP}(\phi) = \frac{T_6[1 - (\xi_{HX}\phi)^{(1-\gamma)/\gamma}]\eta_t}{(T_3/\eta_c)[\phi^{(\gamma-1)/\gamma} - 1] + \eta_t T_6[(\xi_{HX}\phi)^{(1-\gamma)/\gamma} - 1]}$$

where $\phi = p_2/p_1$, $T_6 = T_{cool}$, $T_3 = T_{reject}$, $\xi_{HX} = (1 - \eta_{HX\,in})(1 - \eta_{HX\,out})(1 - \eta_{rec\,in})(1 - \xi_{rec\,out})$, and γ is the specific heat ratio of the fluid. A 10% total pressure drop is assumed to be split between the heat exchanger and recuperator: $\eta_{reg\,in} = 0.95$, $\eta_{reg\,out} = 0.95$, $\eta_{HX\,in} = 0.95$, and $\eta_{HX\,out} = 0.95$. The COP is plotted as a function of the pressure ratio ϕ in Fig. 9 for several values of γ.

For a given working fluid and cooling temperature, the COP is a function of the rejection temperature and pressure ratio. Analogous to the Rankine, it would be best to express COP as a function of rejection temperature alone. This is achieved in the following manner: from Fig. 10, it can be seen that, corresponding to every rejection temperature, there exists one maximum COP, occurring at a particular pressure ratio. For a given rejection temperature, the maximum value of the COP is chosen and the pressure ratio corresponding to this COP is taken to be the operating pressure ratio. This procedure ensures optimization of COP with respect to pressure ratio, thereby reducing the number of independent variables that COP depends on by one. This procedure was implemented using a Fortran 77 code, and the results for pure helium are plotted in Fig. 11. The COP varies almost linearly with rejection temperature. No interpolation is performed to obtain COP as a function of rejection temperature.

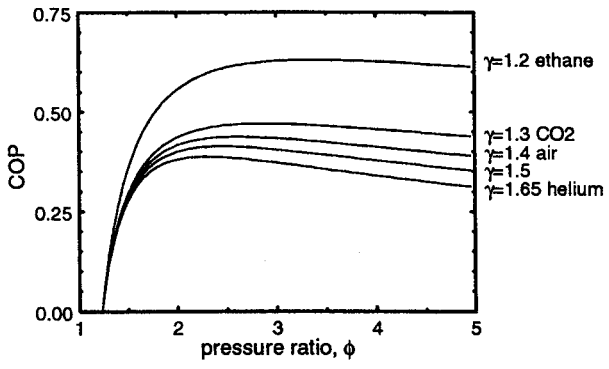

Fig. 9 COP vs ϕ for several values of γ for a recuperated Brayton cycle (T_{reject} = 380 K).

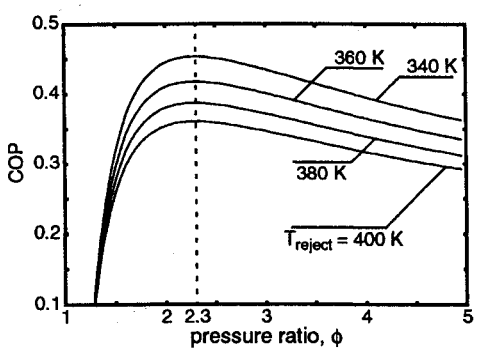

Fig. 10 COP vs ϕ for the recuperated Brayton cycle (γ = 1.65).

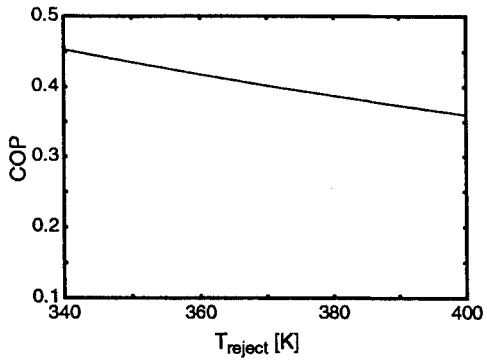

Fig. 11 COP as a function of rejection temperature for the recuperated Brayton cycle (γ = 1.65).

In Fig. 10, note that the maximum COP for the recuperated cycle occurs at a single constant pressure ratio (2.3:1 for helium), irrespective of the condenser temperature. This is because of the assumption of an ideal recuperator, i.e., $T_4 = T_6$.

Selection of a Working Fluid

The desirable properties for the working fluid can be deduced from the results of the previous analysis as follows: lower specific heat ratios γ permit higher coefficients of performance. Therefore, the most obvious decision is to choose a fluid with a low γ. Gases that have low molecular weights have an advantage because of lower friction.[18] However, a lower molecular weight for the working fluid leads to increases in the mass of the processing equipment because of decreased fluid momentum. Working fluids with low specific heats require a larger heat exchanger. A mixture of helium and xenon having a higher molecular weight is preferred because of the reduced mass of the heat exchanger and the recuperator.[18]

Mass Optimization

Input and Output Heat Exchangers

The input heat exchanger transfers heat between the acquisition loop and the heat pump. The output heat exchanger conveys heat between the heat pump loop and the rejection loop. The specific mass of both heat exchangers is 2.72 kg for every kilowatt of heat exchanged.

Recuperator

The recuperator exchanges heat between two gaseous fluids. Hence, the area of the heat exchanger and its mass are large. The specific mass of the recuperator has been estimated at 10 kg for every kilowatt of heat exchanged.[19]

Rotating Machinery

The rotating machinery consists of the turbine, compressor, and a motor mounted on a single shaft. A specific mass of 1 kg for every kilowatt of power driving the turbine shaft is used for this analysis. The efficiencies anticipated are $\eta_t = 0.87$ and $\eta_c = 0.8$ (Ref. 19). This empirical formula is valid in the range of 100–200 kW of shaft power.

Results

For the Rankine cycle, values for COP and the mass of the piping were compared and tabulated for a range of rejection temperatures using the mass models presented previously. These values were imported into a spreadsheet and linearly interpolated where necessary. The mass optimization was performed using the spreadsheet. The radiator temperature, or equivalently the heat pump temperature lift, was varied and the masses of the various components were computed.

Figure 12 depicts an example of the trends involved in the mass optimization. Shown here is case B with R11 as a work-

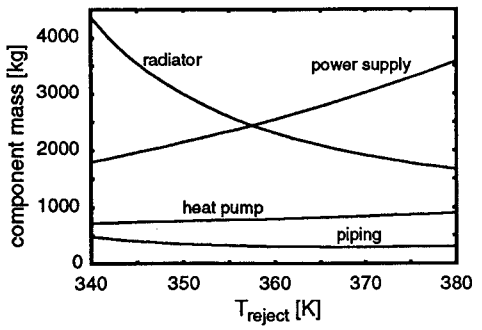

Fig. 12 Component masses for Rankine cycle TCS, case B, with R11.

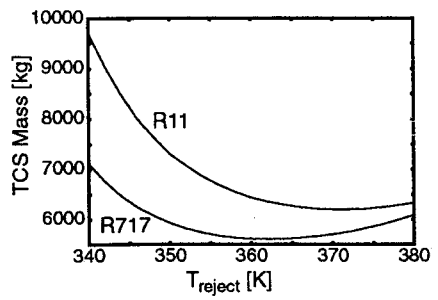

Fig. 13 TCS mass as a function of rejection temperature for case A.

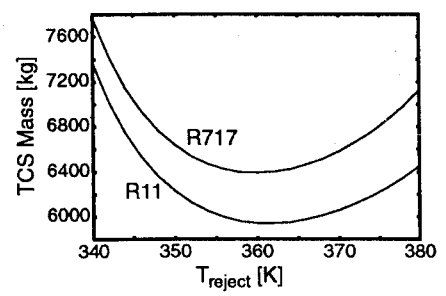

Fig. 14 TCS mass as a function of rejection temperature for case B.

ing fluid and R717 in the rejection loop. The two largest mass fractions are because of the radiator and the power supply. Radiator mass decreases sharply with increasing rejection temperature because of the fourth-power temperature dependence in the Stefan–Boltzmann law. The power supply mass increases with rejection temperature. A higher temperature lift of the heat pump requires more power to be supplied. The opposing trends of the radiator and power supply mass govern the overall mass optimization.

For case A, the analyses were performed for two refrigerants, R11 and R717. The results are shown in Fig. 13. For case B, R11 or R717 was used as the heat pump working fluid and R717 was used as the rejection loop coolant. The results are presented in Fig. 14. When R11 is used as the working fluid for the heat pump, the optimal TCS mass is 6108 kg at a radiator temperature of 371 K for case A. For case B, the optimal TCS mass is 5940 kg at a radiator temperature of 362 K. The radiator mass is higher in case B than in case A because of the lower radiator temperature. In addition, the condenser mass and rejection loop pump mass add to the total TCS mass in case B. However, the superior transport properties of R717 in the rejection loop reduces its mass significantly in case B and results in the overall TCS mass being lower for case B than for case A when R11 is used as the refrigerant. When R717 is used as the working fluid in the heat pump, the optimal mass of the TCS is 5515 kg at a radiator temperature of 362 K for case A. For case B, the corresponding values are 6392 kg and 360 K, respectively. Because of the lower radiator temperature, additional heat exchanger, and rejection loop pump, case B is more massive than case A. Among the cases considered, R717 with the case A configuration has the lowest TCS mass, 5515 kg, followed by 5940 kg for case B with R11 as the heat pump fluid and R717 and the rejection loop coolant. For the additional 425 kg, the latter system offers significant operational and safety improvements and would be the system of choice for Rankine cycle systems.

A mass analysis for the recuperated Brayton cycle TCS has been carried out with air, helium, and ethane as the working fluid. Figure 15 depicts the overall Brayton cycle TCS mass for these working fluids. The TCS mass exhibits a minimum of 14,836 kg at a rejection temperature of 381 K for helium, 13,804 kg at 379 K for air, and 12,789 kg at 374 K for ethane. Figure 16 shows a graphical comparison of the optimal overall TCS masses for the Rankine and Brayton cycle systems. It is found that the Rankine cycle system is less massive than the Brayton cycle system.

Sensitivity analyses have been performed for radiator-specific mass and power penalties. Figure 17 shows the variation

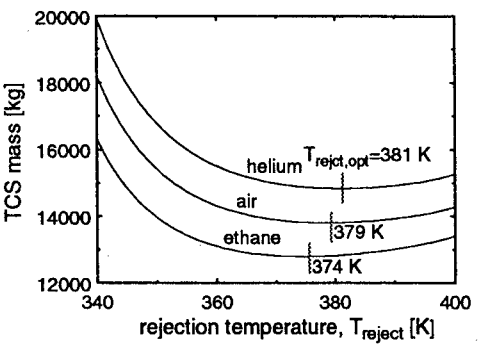

Fig. 15 TCS mass as a function of rejection temperature for helium, air, and ethane.

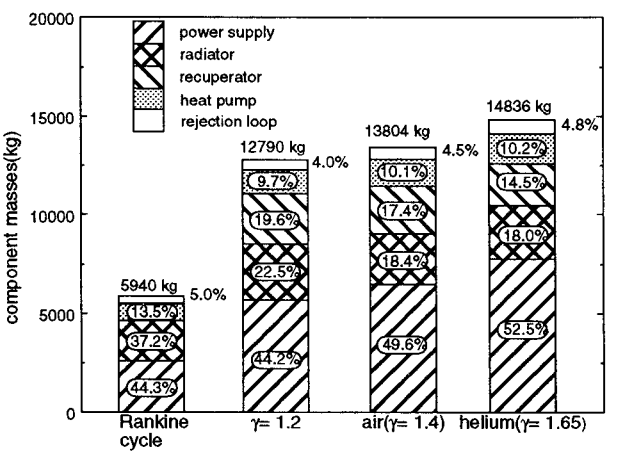

Fig. 16 Overall TCS and component masses for various working fluids.

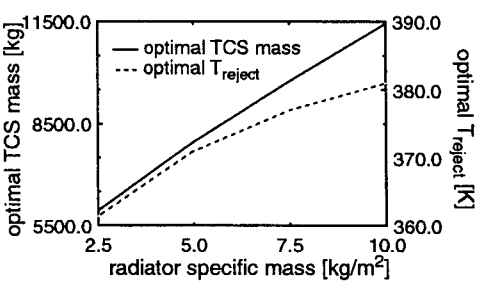

Fig. 17 Sensitivity analysis for radiator-specific mass, case B, R11.

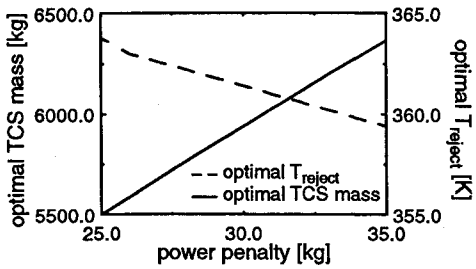

Fig. 18 Sensitivity analysis for power penalty, case B, R11.

of optimal TCS mass and optimal rejection temperature with radiator-specific mass for the Rankine cycle, case B. Since the radiator mass is one of the two largest mass fractions of the TCS, a change in radiator-specific mass has a significant impact on the overall optimal mass. A four-times-larger radiator-specific mass roughly doubles the overall optimal mass. The optimal rejection temperature increases with radiator-specific mass. Figure 18 shows the variation of optimal TCS mass and optimal rejection temperature with power penalty for the Rankine cycle, case B. Here, again, it is found that the optimal TCS mass increases almost linearly with power penalty and the rejection temperature decreases with power penalty. Both these trends can be explained based on Fig. 12. The variation in the heat pump and plumbing masses with rejection temperature is not significant. However, the masses of the radiator and power supply vary significantly with the rejection temperature. An increase in the rejection temperature leads to a sharp decline in the radiator mass and a large increase in the power supply mass because of the increased temperature lift. An increase in the specific mass of the radiator would drive the minimum of the TCS mass to a higher rejection temperature and a large power penalty would push the rejection temperature to a lower value for a minimum TCS mass.

Conclusions

Until other options, such as lunar soil thermal storage and shaded radiators, have been thoroughly analyzed for their performance in the lunar environment, a heat-pump-based TCS is the most suitable concept for moderate-temperature heat rejection on lunar bases. Rankine and Brayton cycle systems were analyzed as candidate cycles for the heat pump. A thorough mass analysis using real properties of refrigerants and real mass models and performances has been performed for the Rankine cycle. The mass of a TCS using a Rankine cycle heat pump that uses R11 as the heat pump fluid and R717 as the rejection loop fluid was identified as the system of choice for this cycle. Such a cycle rejected 100 kW of lunar base heat at 270 K to the lunar environment by raising the effective radiator temperature to 362 K. The total mass of this TCS was 5940 kg. This case was used as the benchmark.

A Brayton cycle heat pump TCS was considered next. The mass of the optimal system, 12,970 kg at a radiator temperature of 374 K, was found to be more than twice that of the optimal Rankine system.

Acknowledgments

This research was supported by NASA Goddard Space Flight Center under Grant NAG5-1572. We would like to express our gratitude to Ted Swanson of GSFC for his support and many valuable suggestions and ideas. We are also grateful to Ashok Nanjundan for his assistance with the Brayton cycle analysis.

References

[1]Cremers, C. J., Birkebak, R. C., and White, J. E., "Lunar Surface Temperatures from Apollo 12," *The Moon*, Vol. 3, No. 3, 1971, pp. 346–351.

[2]Simonson, L. C., DeBarro, M. J., Farmer, J. T., and Thomas, C. C., "Conceptual Design of a Lunar Base Thermal Control System," Symposium on Lunar Base and Space Activities in the 21st Century, Paper LBS-88-225, Houston, TX, April 1988.

[3]Ewert, M. K., Petete, P. A., and Dzenitis, J., "Active Thermal Control Systems for Lunar and Martian Exploration," Society of Automotive Engineers Paper 901243, July 1990.

[4]Swanson, T. D., Rademacher, R., Costello, F. A., Moore, J. S., and Mengers, D. R., "Low-Temperature Thermal Control for a Lunar Base," Society of Automotive Engineers Paper 901242, July 1990.

[5]Costello, F. A., and Swanson, T. D., "Lunar Radiators with Specular Reflectors," *Heat Transfer in Space Systems*, edited by S. H. Chan, E. E. Anderson, R. J. Simoneau, C. H. Chan, D. W. Pepper, and B. F. Blackwell, American Society of Mechanical Engineers, HTD-Vol. 135, New York, 1990, pp. 145–150.

[6]Ewert, M. K., "Investigation of Lunar Base Thermal Control System Options," Society of Automotive Engineers Paper 932112, July 1993.

[7]Sridhar, K. R., and Gottmann, M., "Thermal Control Systems for Low-Temperature Heat Rejection on a Lunar Base," Final Rept., Grant NAG5-1572, NASA/GSFC, Oct. 1992.

[8]Waldron, R. D., "Lunar Base Power Requirements, Options and Growth," *Proceedings of Space 90*, American Society of Civil Engineers, Albuquerque, NM, 1990, pp. 1288–1297.

[9]Reynolds, W. C., "Thermodynamic Properties in SI," Dept. of Mechanical Engineering, Stanford Univ., Stanford, CA, 1979.

[10]Gottmann, M., and Sridhar, K. R., "Thermal Control Systems for Low-Temperature Heat Rejection on a Lunar Base," *28th International Heat Transfer Conference*, American Inst. of Chemical Engineers, San Diego, CA, 1992, pp. 148–157.

[11]"Carrier System Design Manual; Part 3: Piping Design," Carrier Air Conditioning Co., Syracuse, NY, 1973.

[12]Dexter, P. F., and Haskin, W. L., "Analysis of Heat Pump Augmented Systems for Spacecraft Thermal Control," AIAA Paper 84-1757, June 1984.

[13]Guerra, L., "A Commonality Assessment of Lunar Surface Habitation," *Proceedings of Space 88*, American Society of Civil Engineers, Albuquerque, NM, 1988, pp. 274–288.

[14]Drolen, B., "Heat Pump Augmented Radiator for High Power Spacecraft Thermal Control," AIAA Paper 89-0077, Jan. 1989.

[15]Juhasz, A. J., and Bloomfield, H. S., "Development of Lightweight Radiators for Lunar Based Power Systems," NASA TM 106604, June 1994.

[16]Landis, G. A., Bailey, S. G., Brinker, D. J., and Flood, D. J., "Photovoltaic Power for a Lunar Base," *Acta Astronautica*, Vol. 22, 1990, pp. 197–203.

[17]Roschke, E. J., and Wen, L. C., "Preliminary System Definition Study for Solar Thermal Dynamic Space Power Systems," Jet Propulsion Labs., TR D-4286, Pasadena, CA, June 1987.

[18]Wood, B. D., *Applications of Thermodynamics*, 2nd ed., Waveland Press, Inc., Prospect Heights, IL, 1991.

[19]Juhasz, A., private communication, NASA Lewis Research Center, Hampton, VA, Dec. 1992.